

	Page
Problems in Hazard Analysis and Risk Assessment by N.C. Harris	267
Process Safety Analysis: Identification of Inherent Process Hazards by C.A.W.A. Husmann and T. Van de Putte	285
Bulk Storage of LPG – Factors Affecting Offsite Risk by M. Considine, G.C. Grint and P.L. Holden	291
Hazard Assessment of Layout by J.C. Mecklenburgh	321
Siting and Layout of Major Hazardous Installations by C.G. Ramsay, R. Sylvester-Evans and M.A. English	335
Development of Low-cost Risk Analysis Methods for Process Plant by R.A. Cox and P.J. Comer	353
An Example of HSE's Assessment of Major Hazards as an Aid to Planning Control by Local Authorities by Dr. M.F. Pantony and Dr. L.M. Smith	377
Thermal Radiation Hazards From Large Pool Fires and Fireballs – A Literature Review by J. Moorhouse and M.J. Pritchard	397

A REVIEW OF MATHEMATICAL MODELS FOR PREDICTION  
OF HEAVY GAS ATMOSPHERIC DISPERSION

J. A. Havens\*

Mathematical models for atmospheric dispersion of heavy gases are reviewed. Treatment of gravity spreading of heavy gas clouds and air entrainment are emphasized. Considerable variation in the methods of treatment of air entrainment is identified. The importance of gravity spreading compared to atmospheric turbulence-generated lateral spreading is considered, and a criterion is suggested for evaluation of their relative importance. Several heavy gas dispersion tests which have been conducted appear to have been dominated by atmospheric turbulence and hence provide little basis for extrapolation to catastrophic releases where gravity-driven flows are expected to dominate.

INTRODUCTION

Risk of accidental release of heavier-than-air gases accompanies many manufacturing, storage and transportation operations. Although increased public attention to such risks reflects, in large part, extensive debate on the risks associated with marine transport of very large quantities of flammable liquefied gases (1,2,3), many other potentially hazardous chemicals can produce heavy gas or aerosol "clouds" when released into the atmosphere (4,5). Assessment of risk attending such operations invariably involves estimation of the probability of release and the ensuing atmospheric dispersion, since such dispersion eventually results in dilution of the gas with air to concentrations which are non-flammable (or non-explosive) or within acceptable toxicity limits. Therefore, a prediction of the location of the "boundary" of such clouds (defined, for example, as containing gas concentrations above a prescribed lower concentration limit) with respect to time is required for rational risk assessment.

Considerable effort has been directed to the understanding of heavy gas atmospheric dispersion in the last ten years. The purpose of this paper is to summarize these developments in some historical perspective and to present a view of the state of our understanding of the problem.

BACKGROUND

The recognition of the need for a more quantitative understanding of heavy gas dispersion processes was in part a result of extensive debate regarding the risks associated with marine transport of liquefied natural gas (LNG).

\*Department of Chemical Engineering, University of Arkansas, Fayetteville AR 72701 USA.

The marine carriage of LNG at approximately 112° K in individual tanks of approximately 25,000 m<sup>3</sup> volume portends the possibility of rapid release of a very large quantity of LNG if catastrophic tank failure should occur in a collision (6). Risk analyses performed in support of requests for regulatory permits to build and operate LNG ships and the associated terminals required (along with other indices of risk) predictions of the maximum downwind distance to the lower flammable limit following the release of cargo tank volumes of LNG under applicable atmospheric and sea surface conditions. There were order of magnitude variations in these predictions (7), which were in part due to lack of standardization of spill/atmosphere conditions simulated, but which also reflected different modeling approaches to the problem.

The process of dispersion of heavy gases following accidental release into the atmosphere differs importantly from the process of dispersion of trace contaminants in the atmosphere. The theory underlying prediction of atmospheric dispersion of trace contaminants (pollutant dispersion) generally assumes that the dispersion is the result of the turbulent motion (which induces mixing) that characterizes the atmospheric boundary layer. The presence of the pollutant is consequently assumed not to affect the atmospheric flow patterns, with the result that the problem becomes one of understanding and prediction of atmospheric boundary layer turbulence. Although the characterization of atmospheric flow suffers from the general limits to our understanding of turbulent fluid motion, there exists a fairly well developed theoretical basis for prediction of the dispersion of trace contaminants in the atmosphere, along with extensive supporting experimental data derived from atmospheric flow measurements (8).

In contrast, the accidental release of large quantities of heavy gases into the atmosphere may alter the fluid flow pattern in the atmosphere in the vicinity of the release. The subsequent heavy gas motion and mixing with air then involves complex interaction of the flows existing in the atmosphere prior to the release and the flow of the heavy gas, which may be strongly influenced by gravitational forces. For large quantity releases the gravity-induced flow and the resulting interaction with the atmospheric flow can determine the shape and extent of the area which is exposed to flammable or toxic gas concentrations. The early phases of cloud formation, motion and dispersion following release of large quantities of heavy gases involve density-stratified flows which are not well understood (9).

#### MATHEMATICAL MODELS

During the decade 1970-1980 a number of mathematical modeling techniques for predicting heavy gas dispersion were published. These models, which in most cases appear to have been developed for risk assessment studies of liquefied gas fuel importation projects in the U.S. and Europe, can be (somewhat arbitrarily) classified in two categories.

1. Box or "top hat" profile models which represent the initial development of the cloud (in the case of an instantaneous release) or a cross-sectional slice of the cloud (in the case of a steady continuous release) as a uniformly mixed volume. The shape, thermodynamic properties and position of the cloud are modeled using correlations derived for the velocity of density intrusions and fluid entrainment across density interfaces. This model type often incorporates a transition, usually to a gaussian model, to describe passive dispersion (controlled by atmospheric turbulence) of the gas in the far field.

2. K-theory models which assume constitutive relations between turbulent fluxes and the gradients in mean variables velocity, temperature and concentration, coupled with the equations of change for mass, momentum and energy for turbulent fluid flow to predict the time and spatial variation of the thermodynamic properties of the cloud.

Recent models overlap these categories. The assumption of a self-similar solution allows representation of the concentration in the form

$$c(x,y,z) = c_s f(x/x_s, y/y_s, z/z_s)^* \quad (1)$$

Several investigators (10,11,12) have assumed self-similar concentration profiles in the form

$$c(x,y,z) = c_s(x) \exp \left[ - \left( \frac{y}{y_s} \right)^a - \left( \frac{z}{z_s} \right)^b \right] \quad (2)$$

and some have coupled the assumption of a self-similar concentration profile with a K-theory representation of turbulent mass transfer within the cloud (11).

More recently there have appeared several models which involve greater simplification of the equations of motion, energy and mass than is found in the K-theory models, but which still require solution of partial differential equations to predict cloud state variables. Models proposed by Zeman (13), Rosenzweig (14) and Fanelop (15) are not described here due to their recent introduction but may represent significant advantages over the box models since they allow a more realistic representation of spatial variation in the simulation of cloud dispersion, and incorporate more general turbulent mixing sub-models.

It appears that some of the models reviewed by Havens (7) in 1977 have been recognized as inadequately describing essential features of the heavy gas dispersion process now widely recognized (16). However, others continue to be used in risk assessment studies for proposed liquefied gas fuel import terminals in the United States, Europe and Japan as well as for assessment of the potential risk of heavy gas cloud formation at existing chemical and petrochemical complexes and in the transportation of fuels and chemicals. There is still substantial disagreement among the models currently in use.

#### Box (Top Hat Profile) Models

A number of models have been proposed in this category, but it is possible to consider a general form in which different approaches have been undertaken to the modeling of gravity spreading and air entrainment into the well mixed volume or cloud.

Since the model assumes uniform thermodynamic properties, its use is restricted to the representation of two types of heavy gas clouds.

\*The box model could be viewed as representing the simplest form for  $f$ , i.e.

$$f(y/y_s, z/z_s) = 1 \quad \text{for } y < y_s, \quad z < z_s$$

$$\text{and } f(y/y_s, z/z_s) = 0 \quad \text{for } y > y_s, \quad z > z_s$$

1. An instantaneously released quantity of gas with a known initial volume, usually represented as a vertically oriented cylinder whose radial and height dimensions change as a result of gravity spreading and air entrainment across the outer "surfaces" of the cloud. The cylindrical cloud is usually assumed to be translated with the wind.
2. A steady plume with rectangular cross section (axis along the wind direction) whose thermodynamic properties vary with downwind position and whose width and height change as a result of gravity spreading (assumed to occur laterally only) and air entrainment across the outer surfaces.

In either case the model requires analytical expressions for the spreading velocity (i.e. the velocity of the cloud edge) and the entrainment of air at the cloud boundaries.

All proponents of this approach have modeled the velocity of the cloud edge as a density intrusion (17) using the relation

$$u_f = \alpha_1 \left[ g \left( \frac{\rho_g - \rho_a}{\rho_g} \right) h \right]^{1/2} = \alpha_1 [g\Delta h]^{1/2} \quad (4)$$

$$\text{or } u_f = \alpha_1 \left[ g \left( \frac{\rho_g}{\rho_a} - 1 \right) h \right]^{1/2} = \alpha_1 [g\Delta' h]^{1/2} \quad (5)$$

where the Boussinesq approximation, or neglect of inertial effects of density variations, is invoked in Equation 5.

The density of the cloud, which is treated as spatially uniform in the box models, is affected by energy transfer from the cloud surroundings as well as the entrainment of air into the cloud. Some of the box models provide for heat transfer to the cloud from the earth's surface. We purposely exclude consideration of the different approaches to modeling the surface-to-cloud heat transfer in this paper to focus on the treatment of gravity spreading and entrainment modeling. It is probable, however, that such heat transfer may importantly affect the dispersion of cryogenic gases such as LNG, and some investigators have indicated that air entrainment may be significantly enhanced due to convection-generated turbulence (13,18). Analysis of the DOE China Lake LNG spill test data, which is not yet available at the time of writing, may provide information in this regard, since data sufficient to perform energy balance analyses on the cloud should be available.

Although modeling of the air entrainment has been treated differently by investigators, all of the box models can be represented as requiring entrainment velocities which are used in the general form

$$\dot{V}_a = w_e A_T + u_e A_F \quad (6)$$

where  $A_T$  and  $A_F$  are cloud top and frontal areas and  $w_e$  and  $u_e$  are vertical and horizontal entrainment velocities respectively.

There exists little guidance on the evaluation of  $u_e$  for large ratios of  $A_F/A_T$ , i.e. during the early phase of the gravity spreading process, but in

models where it has been included the horizontal entrainment velocity has either been modeled as

$$u_e = c_f u_f \quad (7)$$

$$\text{or } u_e = \frac{c_f u_f^2}{u_f(t=0)} \quad (8)$$

Equation 8, proposed by Eidsvik (19) reduces to Equation 7 in the limit  $t \rightarrow 0$ , but gives an effective horizontal entrainment coefficient which decreases to zero for  $A_T/A_F \gg 1$ .

Vertical entrainment (mixing) of air into a density-stratified heavy gas layer would be expected to be a function of a characteristic vertical turbulence velocity (such as a friction velocity) and the stabilizing effect of the density gradient relative to the shear flow. If the heavy gas flow is viewed as being superimposed on the local atmospheric flow and convection-induced turbulence is neglected, characteristic vertical turbulence velocity can be represented as a friction velocity for the flow where

$$u_* = \left( \frac{1}{2} C_F \right)^{1/2} u \quad (9)$$

$C_F$  is a surface-friction drag coefficient and  $u$  is a characteristic wind velocity  $u_a$ , or, as represented in some models, the vector sum of the gravity spreading velocity and the characteristic wind velocity

$$u^2 = u_g^2 + u_a^2 \quad (10)$$

The vertical density stratification of the flow is measured by a form of the overall Richardson Number

$$Ri = \frac{g\Delta h}{u_*^2} \quad \text{or} \quad \frac{g\Delta' h}{u_*^2} \quad (11)$$

Classical boundary layer analysis (20) suggests that in the constant stress layer of the atmosphere, the vertical entrainment velocity should be proportional to the friction velocity in the absence of stratification and should be inversely proportional to the Richardson number for stratified flow.

$$w_e = c_1 u_* \quad (Ri \rightarrow 0) \quad (12)$$

$$w_e = c_2 u_* / Ri \quad (Ri > 0) \quad (13)$$

Equations 12 and 13 are applicable to entraining boundary layers adjacent to the earth's surface and reflect momentum transfer toward the solid boundary.

Velocity shear is also produced at the fluid-fluid interface between a spreading heavy gas layer and the overlying atmospheric flow. Turbulent mixing across such a cloud top surface can result due to breaking waves associated with unstable flow generated at the interface (9). Some heavy gas cloud models have provided for air entrainment via this mechanism, with the entrainment assumed proportional to the difference in velocity across the interface. For a spreading "top hat profile" gas layer, such entrainment is given by

$$w_e = c_3(u_g - u_a) \quad (14)$$

In the following, a brief summary of the approaches which have been proposed (chronologically) for air entrainment modeling in top hat models is given.

Van Ulden (21) characterized the heavy gas flow with the Richardson Number  $Ri = g\Delta h/u_*^2$  with  $u_*$  representing the friction velocity of the atmospheric flow. He suggested that cloud frontal entrainment is very small, if not negligible, and that cloud top entrainment during the gravity-dominated spread phase, which he defined as  $Ri \gg 4/\alpha_1^2$ , is also negligible. Thus Van Ulden's model of the gravity spread phase indicates minimal cloud volume growth (and dilution) given by

$$\dot{V}_a = \dot{V} = u_e A_F = 0.05 u_f A_F \quad (15)$$

Van Ulden suggests that atmospheric turbulence-induced mixing will begin to control when the spreading velocity has been reduced to  $2 u_*$  ( $Ri = 4/\alpha_1^2$ ) and thereafter models the cloud dilution using a classical gaussian passive dispersion model. It appears that Van Ulden's model entrainment parameters were based primarily on analysis of the growth of a heavy Freon-air cloud following essentially instantaneous vaporization of 1000 kg liquid Freon dumped into water. It is important to note that measurements of the initially formed visible cloud indicated a rapid, initial, ten-fold dilution of the Freon, and Van Ulden modeled the subsequent dispersion only.

Germesles and Drake (22) neglect cloud frontal entrainment and model top entrainment using Equation 14. Germesles and Drake suggest  $c_3 = 0.1$  based on their Froude Number extrapolation of Lofquist's data (23) for entrainment coefficients for mixing across a density/shear interface between a salt water flow and overlying quiescent pure water. The flow in Lofquist's experiments was three-dimensional (the flow was in a channel with comparable width and depth) and although Lofquist's correlation of the data utilized a Froude number which incorporated the hydraulic radius of the heavy layer, this appears not to have been accounted for in Germesles' and Drake's extrapolation. Our analysis indicates an order of magnitude uncertainty in the value of the entrainment coefficient inferred from the Germesles-Drake extrapolation if the geometry of the flow is taken into account. It should also be noted that the top entrainment coefficient of 0.1 inferred by Germesles and Drake is sensitive to the value of  $\alpha_1$  in the front spreading velocity equation (Equation 5). If  $\alpha_1 = 1.0$  is assumed, in contrast to  $\alpha_1 = 2^{1/2}$  as suggested by Germesles-Drake, their extrapolation gives  $c_3 = 0.01$  at the front velocity. Finally, the extrapolated value of  $c_3 = 0.1$  would appear, in any case, to be applicable only to the top area near the cloud front (since it reflects the Froude number at the front) and should be smaller for those areas of the cloud top which are spreading at lower velocity.

Picknett (24) correlated the concentration and visible cloud dimensioing data from a series of instantaneous releases on land of approximately 40 m of Freon-air mixtures ranging in relative density ( $\rho_g/\rho_a$ ) from about 2.0 to 5.0. Picknett fitted the large initial entrainment inferred from the data using the frontal entrainment relation (Equation 7) with  $c_f = 0.82$ . He modeled top entrainment using Equation 13 with  $c_2 = 0.15$ . Picknett terminates the gravity spreading phase, and transitions to a gaussian passive dispersion model, when the Richardson number of the spreading layer decreases to  $Ri = 7$ .

Eidsvik's top hat model (19) does not transition to a gaussian passive dispersion model. Instead, the model uses air top entrainment relations incorporating Equation 13 (which controls during the early gravity spread

phase when  $Ri \gg 1$ ) and Equation 12 (which controls during the later phase of the cloud dilution when density-driven flows have subsided, as indicated by  $Ri \rightarrow 0$ ). However, Eidsvik's model utilizes a different form of the friction velocity and Richardson Number to describe the flow. Incorporating Eidsvik's suggested model parameter values, his equation for vertical entrainment is

$$w_e = \frac{w}{3.33 + 0.29 Ri'} \quad (16)$$

which in the absence of thermal convection effects (Eidsvik includes recommended measures of convective turbulence velocities also, but these effects are not considered here) is given by

$$w = 1.3 u_*' \quad (17)$$

$$\text{and } u_*' = \left(\frac{1}{2} C_F\right)^{1/2} u$$

where  $C_F$  is a surface drag coefficient and  $u$  is calculated as the vector sum of the average gravity flow velocity and the average wind speed

$$u^2 = (\eta u_f)^2 + u_a^2 \quad (18)$$

and the constant  $\eta$  is dependent on the geometry of flow ( $\eta = 2/3$  for axisymmetric and  $1/2$  for one-dimensional spreading). The Richardson Number  $Ri'$  is then defined as

$$Ri' = \frac{g\Delta h}{w^2} \quad (19)$$

Using Equations 4, 17 and 18 the Richardson number  $Ri'$  can be expressed as

$$Ri' = \frac{0.59 u_f^2}{\alpha_1^2 (1/2 C_F) ((\eta u_f)^2 + u_a^2)} \quad (20)$$

In the limit as  $u_f/u_a \ll 1$ , this Richardson number approaches

$$Ri' \Big|_{u_f \ll u_a} = \frac{1.18 (u_f/u_a)^2}{C_F \alpha_1^2} \quad (21)$$

and  $w_e$  approaches

$$w_e \Big|_{u_f \ll u_a} = 0.39 (1/2 C_F)^{1/2} u_a \quad (22)$$

which is consistent with the assumed dependence of  $w_e$  on  $u_*$  given by Equation 12.

For  $u_f \gg u_a$ , however, Eidsvik's Richardson Number  $Ri'$  is approximately

$$Ri' \Big|_{u_f \gg u_a} = \frac{1.18}{C_F \alpha_1^2 \eta^2} \quad (23)$$

and  $w_e$  approaches (for  $C_F \ll 1.0$ ,  $\alpha = 1.3$ , and  $\eta = 2/3$ )

$$\frac{w_e}{u_f} \Big|_{u_f \gg u_a} \approx 0.47 C_F^{3/2} u_f \quad (24)$$

Eidsvik cites recommended values for  $C_F$  of  $2 \times 10^{-3}$  for flow over water and  $1.4 \times 10^{-2}$  for flow over land. For this range, and with  $\alpha_1 = 1.3$ ,  $\eta = 2/3$ ,  $w_e$  given by Equation 24 varies between  $0.00004 u_f$  and  $0.0008 u_f$ . It should be noted that Eidsvik's limiting (as  $u_f \gg u_a$ ) entrainment expression of Equation 24, with a coefficient of order  $10^{-4}$  to  $10^{-3}$ , infers a different entrainment mechanism from that of Germeles' and Drake's suggested entrainment relation (Equation 14). Eidsvik's model neglects entrainment due to shear at the interface (he indicates that Kelvin-Helmholtz instability might provide a mechanism for such entrainment, but assumes it to be effectively damped out because of the strong density stratification across the interface) whereas Germeles' and Drake's suggested entrainment is associated with the shear at the interface. Equation 24 then must be viewed as a prescription for vertical entrainment associated with shear at the earth's surface, which is, for  $u_f \gg u_a$ , still identified with a surface boundary layer friction velocity.

Cox and Carpenter (25) recommended modeling frontal entrainment using Equation 7 with  $c_f = 0.6$  and top entrainment using the following expressions

$$\begin{aligned} w_e &= 0.15 u_1 \quad \text{for } Ri'' \rightarrow 0 \\ w_e &= 0.1 u_1 / Ri'' \quad \text{for } Ri'' \gg 1 \end{aligned} \quad (25)$$

where  $u_1$  is the horizontal r.m.s. turbulence velocity of the wind flow and  $Ri''$  is defined as

$$Ri'' = \frac{g \Delta' L}{u_1^2} \quad (26)$$

$u_1$  is assumed to be proportional to  $u_*$ , so that

$$u_1 = \left( \frac{u_1}{u_*} \right) u_* \quad (27)$$

Values of  $u_1/u_*$ , attributed to Pasquill (8) of 3.0, 2.4, and 1.6 for very unstable, neutral and very stable atmospheric flows respectively, are used. The turbulence scale length  $L$  is correlated with height above ground (cloud depth) and atmospheric stability using data from Taylor et al. (26). Using the suggested values for  $u_1/u_*$  along with estimates of  $L/h$  from Taylor et al., Equations 25 can be rewritten in the form of Equations 12 and 13 with a stability-dependent proportionality constant.

Table 1 summarizes the top hat profile gravity spreading and air entrainment sub-models.

Advanced "Similarity" Models

Models which assume gaussian forms for the concentration profiles in a developing heavy gas cloud or plume have been proposed by te Riele (10), Flothmann and Nikodem (12), Ooms (28), and Colenbrander (11). We consider here only the Colenbrander model, which provides for quasi-steady

TABLE 1 - Top Hat Profile Model Gravity Spreading and Entrainment Parameters

	Spreading Model	Frontal Entrainment Velocity	Cloud Top Shear	Top Entrainment Velocity	
				$u_f \gg u_a$	Earth Surface Boundary Layer Shear $u_a \gg u_f$
Van Uliden (1974)	$u_f = 1.0 (g\Delta h)^{1/2}$	$0.05 u_f$	None	None	transition to gaussian model at $Ri = 4 (u_f = 2u_*)$
Germeles-Drake (1975)	$u_f = 1.41 (g\Delta' h)^{1/2}$	None	$0.1 u_g$	None	transition to gaussian model at $Ri = 2/C_F \alpha_1^2 (u_f = u_a)$ [1]
Picknett (1978)	$u_f = 0.94 (g\Delta' h)^{1/2}$	$0.82 u_f$	None	$0.15 u_*/Ri$	transition to gaussian model at $Ri = 7$
Eidsvik (1979)	$u_f = 1.3 (g\Delta h)^{1/2}$	$0.5 u_f/u_{f0}$	None	$4.5 u_*/Ri'$	$0.39 u_*$
Cox-Carpenter (1980)	$u_f = 1.0 (g\Delta' h)^{1/2}$	$0.6 u_f$	none	$3.0 u_*/Ri$ [2] $2.0 u_*/Ri$ [3] $0.7 u_*/Ri$ [4]	limiting value of $0.45 u_*$ [2] $0.36 u_*$ [3] $0.24 u_*$ [4] and transition to gaussian model when $u_f = d \sigma_y/dt$

[1] Arthur D. Little Company has suggested a different criterion, for determining transition, which is related to velocity fluctuation magnitude in the atmosphere flow. (27)

[2] For atmosphere stability class (Pasquill-Gifford) B - (unstable)

[3] For atmosphere stability class (Pasquill-Gifford) D - (neutral)

[4] For atmosphere stability class (Pasquill-Gifford) F - (stable)

representation of a heavy gas plume formed downwind of an area source. The model assumes similarity profiles for the concentration and horizontal velocity as follows:

$$c(x,y,z) = c_A(x) \exp \left[ - \left( \frac{|y| - b(x)}{s_y(x)} \right)^2 - \left( \frac{z}{s_z(x)} \right)^{1+\alpha} \right] \quad \text{for } |y| > b \quad (28)$$

$$= c_A(x) \exp \left[ - \left( \frac{z}{s_z(x)} \right)^{1+\alpha} \right] \quad \text{for } |y| \leq b \quad (29)$$

$$u_x = u_0 \left( \frac{z}{z_0} \right)^\alpha \quad (30)$$

We consider here only the method of specifying gravity spreading and vertical entrainment. Vertical turbulent diffusion is modeled via the two-dimensional diffusion equation

$$u_x \frac{\partial c}{\partial x} = \frac{\partial}{\partial z} \left( K_v \frac{\partial c}{\partial z} \right) \quad (31)$$

with a turbulent diffusivity given by

$$K_v = \frac{k u_* z}{\phi(Ri_*)} \quad (32)$$

Substitution of Equations 29, 30, and 32 into Equation 31 gives an expression for  $s_z$  as a function of downwind distance  $x$

$$\frac{ds_z}{dx} = k \frac{u_* (1+\alpha)}{u_0 \phi(Ri_*)} \left( \frac{z_0}{s_z} \right)^\alpha \quad (33)$$

An "effective" depth of the concentration profile is defined as

$$h_{\text{eff}} = \frac{1}{c_A} \int_0^\infty c \, dz = \frac{\Gamma(1/1+\alpha)}{1+\alpha} s_z \quad (34)$$

and an "effective" cloud advection velocity is defined as

$$u_{\text{eff}} = \frac{\int_0^\infty c u_x \, dz}{\int_0^\infty c \, dz} = u_0 \left( \frac{s_z}{z_0} \right)^\alpha \frac{1}{\Gamma \left( \frac{1}{1+\alpha} \right)} \quad (35)$$

Combining Equations 33-35

$$\frac{dh_{\text{eff}}}{dx} = \frac{k u_*}{u_{\text{eff}} \phi(Ri_*)} \quad (36)$$

$$\text{or } \frac{dh_{\text{eff}}}{dt} = w_e = \frac{k u_*}{\phi(Ri_*)} \quad (37)$$

with the overall Richardson number defined as  $Ri_* = g\Delta' h_{\text{eff}} / u_*^2$ .

Equation 37 is of the form discussed earlier for box model entrainment models. Colenbrander used laboratory turbulent entrainment data of McQuaid (29), Kato and Phillips (30), and Kantha, Phillips and Azad (31) to curve fit the function  $\phi(Ri_*)$  as follows

$$\phi(Ri_*) = 0.74 + 0.25 Ri_*^{0.7} + 1.2 \times 10^{-7} Ri_*^3 \quad (38)$$

for positive values of  $Ri_*$ .

Lateral gravity spreading of a plume downwind of the source is modeled using a variant of the density intrusion formula

$$\frac{dB}{dx} = \frac{dB}{dt} u_{\text{eff}}^{-1} = \alpha_1 (g\Delta' h_{\text{eff}})^{1/2} u_{\text{eff}}^{-1} \quad (39)$$

$$\text{with } B = b + \sqrt{\pi} / 2 s_y$$

The parameter  $b$  is the width of the horizontally uniform central section of the plume, and  $s_y$  is a measure of the width of the gaussian-distributed plume edge section, with  $B$  then representing an effective width. Colenbrander suggests a value of  $\alpha_1 = 1.0$ .

#### K-Theory Models

The SIGMET model has been described by Havens (32). Although there have been claims of greatly improved computational methods leading to much reduced running time and expense by the developers of SIGMET (33) and its successor models ZEPHYR and MARIAH (34,35), it is the author's understanding that the specification of turbulent mixing (as well as other physical models used) have not been importantly changed.

"Local" vertical diffusivity is computed using the relation

$$K_v = c_4 \sigma_w k_m^{-1} \quad (40)$$

proposed by Hanna (36), where  $\sigma_w$  is the standard deviation of the vertical fluctuations of the wind velocity,  $k_m$  is the wave number at which the turbulent energy is maximum, and  $c_4$  is a constant. Combining Equation 40 with the following relations proposed by Lumley and Panofsky (37) for neutrally stable conditions in the constant stress layer

$$K_v = 0.4 u_* z \quad (41)$$

$$\sigma_w = 1.3 u_*$$

$$k_m = 0.3 z^{-1}$$

gives

$$K_v = 0.09 \sigma_w k_m^{-1} \quad (42)$$

Based on their analysis of data reported by Taylor et al. (24), SAI assumes the atmospheric turbulence length and  $k_m$  to be (for  $10 < z < 1300$  m)

$$L k_m = 0.2 \quad (43)$$

Representing  $\sigma_w = u \sigma_e$ , where  $\sigma_e$  is the standard deviation of wind direction, it follows that

$$K_v = 0.45 \sigma_e L u$$

SAI represented  $\sigma_e$  and  $L$  as functions of height above ground and atmospheric stability using data from Smith and Niemann (38) and Taylor et al. (26) respectively, with  $K_v/u$  ultimately represented as a function of height and atmospheric stability as shown in Figure 1. Local specification of  $K_v$  in the dispersing heavy gas cloud is then done by computing the local vertical temperature gradient (or an "equivalent temperature gradient" for a density-stratified isothermal cloud) and designating a "local" Pasquill-Gifford stability category therefrom using Table 2.

TABLE 2 - Correlation of Pasquill Stability Categories with Vertical Temperature Gradient (as Used in SIGMET)

$\Delta T/\Delta z$ ( $^{\circ}\text{K}/100$ m)	Stability Class
< -1.9	A
-1.9 to -1.7	B
-1.7 to -1.5	C
-1.5 to -0.5	D
-0.5 to 1.5	E
1.5 to 4.0	F
> 4.0	G

At the time the SIGMET code was described by Havens (32), values of  $K_v/u$  were assumed constant below the 10 meter height, and local velocity was delimited (for use in estimating  $K_v$ ) at a lower value of  $u = 1$  m/sec. Since the results of the SIGMET prediction appear to be controlled by vertical diffusion specification and relatively insensitive to specification of the horizontal dispersion coefficients (32), it is instructive to compare the vertical diffusivity used in SIGMET with the vertical entrainment methods used in the top hat profile and Colenbrander models.

#### Comparison of Entrainment Model Parameter Estimation Methods

The gravity spreading and entrainment model parameters summarized in Table 1, Equations 37-38, and Figure 1 are based on very sparse data. The relatively consistent specification of the spreading equation parameter  $\alpha$  in Equations 4 and 5, accompanied by wide variation in the entrainment sub-models suggested reflects the fact that for adiabatic mixing of air and most heavy gases at constant pressure the buoyancy does not vary greatly. Since most of the field and laboratory heavy gas spread data that has been used to estimate

the constant  $\alpha_1$  in Equations 4 and 5 is derived from measurements of cloud width (usually from overhead photography), the determination of  $\alpha_1$  is insensitive to the degree of vertical mixing (which is reflected in the cloud depth). The widely different entrainment sub-model parameters recommended reflect reliance on different data sets which are difficult to compare. For example, it appears that the use of the Porton Downs instantaneous release data can only be modeled, using the approaches suggested, by incorporating significant frontal entrainment during the initial phase of the spread process, whereas the entrainment parameters suggested by Van Ulden reflect analysis of a cloud which has already been diluted by an order of magnitude.

Vertical mixing estimation methods also differ significantly. Figure 2 shows the nondimensionalized vertical entrainment velocity as a function of Richardson Number used in the box models and Colenbrander model. Although direct comparison in Figure 2 must be made with care because of differences in definitions of velocity scales and Richardson Numbers, analysis of Table 1 and Figure 2 indicate considerable variation in the approaches to entrainment modeling.

It is significant that the entrainment specifications of Colenbrander and Eidsvik are based on laboratory data representing a large Richardson Number range and are consistent with the limiting value of  $w_e/u_*$  of about 0.3 for neutrally buoyant atmospheric boundary layer flow. The correlations shown for Picknett and Cox-Carpenter reflect analysis of the Porton 40 m<sup>3</sup> series data and the Porton trials/Gadilla spills (39) data respectively and do not appear consistent with the small scale laboratory data of McQuaid (29), Kato and Phillips (30), and Kantha, Phillips and Azad (31).

The different methods for termination of the gravity spread phase and the method of subsequent modeling via gaussian relations must also be considered. It is probable that the methods which provide a "smooth" transition (Colenbrander and Eidsvik) are less "sensitive" to model parameter fitting using the sparse field data available than those which require a termination of gravity spread and specification of a virtual source for subsequent treatment.

Finally, it is instructive to compare the vertical diffusivities given by Equations 37 and 38 of Colenbrander's model with those prescribed by the SIGMET model. Figure 3 shows vertical profiles of  $K_v$  specified at the same downwind position (~ 2000 m on the cloud travel centerline) and time (~ 2000 sec) for the simulation of a 25,000 m<sup>3</sup> LNG instantaneous release on water in a neutral (D) atmosphere with 2.25 m/sec wind as predicted by the Colenbrander and SIGMET models. The SIGMET vertical diffusivity profile was obtained in a SIGMET simulation described by Havens (32) in which the  $K_v$ 's specified by the method described earlier herein were divided by 10. Although the comparison shown in Figure 3 is for only one time and position within the LNG cloud, it appears to be typical of the vertical diffusivity comparisons for the same simulation at other times and positions. Consequently, it appears that the vertical diffusivity specification in Colenbrander's model, which reflects consistency with laboratory entrainment data in a similar Richardson Number flow regime (the value of  $Ri_*$  computed by the Colenbrander model at the location and time shown in Figure 3 was about 320) are about one order of magnitude smaller than the values prescribed for the same simulation by SIGMET. It has been suggested previously that the SIGMET specification of vertical diffusion coefficients might be high by an order of magnitude (32). When a 25,000 m<sup>3</sup> LNG spill on water in a neutrally stable atmosphere with a 2.25 m/sec wind is modeled with the Colenbrander model, the Eidsvik model, and the SIGMET model with vertical

diffusivities divided by 10 (as shown in Figure 3), all three models give similar maximum downwind distances to the LFL of 5 - 6 km.

#### The Gravity Spreading Process

It is also instructive to examine the heavy gas gravity spreading process separately from the dispersion process involving air entrainment. For isothermal mixing of ideal gases, the buoyancy ( $g\Delta V$ ) is preserved. Further, although mixing of air and cold gases (such as LNG vapor) does not preserve buoyancy, it may not be changed greatly during the initial phases of mixing when gravity spreading is most important.

Consider the steady state release of a gas of density  $\rho_g$ , at a volumetric rate of  $Q_i$ ,  $m^3/sec$ , from a circular source of diameter  $D$ , at ground level into the atmospheric boundary layer. Neglect the importance of the vertical momentum of the gas from the source. Assume the horizontal component of wind velocity over the release is not affected by the heavy gas injection, and assume the wind field to be characterized by an average velocity  $u_a$ . Assume the buoyancy of the gas-air mixture formed remains constant and the emitted gas is accelerated immediately to the average wind velocity. Further, assume there is no gravity spreading immediately over the release, so that the cross-section of the cloud at the downwind edge of the source is approximated as

being of width  $W_o = \frac{\sqrt{\pi}}{2} D$  and  $h = \frac{Q_i}{W_o u_a}$ . Integration of Equation 5 then

gives the cloud width as a function of downwind distance

$$W = \left[ 3\alpha \left( \frac{g\Delta' Q_i}{u_a^3} \right)^{1/2} x + W_o^{3/2} \right]^{2/3} \quad (45)$$

and the rate of lateral spread with respect to downwind distance is

$$\frac{dW}{dx} = 2\alpha \left( \frac{g\Delta' Q_i}{u_a^3} \right)^{1/2} \left[ 3\alpha \left( \frac{g\Delta' Q_i}{u_a^3} \right)^{1/2} x + W_o^{3/2} \right]^{-1/3} \quad (46)$$

Equation 46 represents the spreading rate due to gravitational influences only, and the spreading rate is indicated to be a function of the length scale  $g\Delta' Q_i / u_a^3$ .

For passive atmospheric dispersion downwind of a point source the plume width can be characterized as  $W_t = 2.5 \sigma_y$  where  $\sigma_y$  is the standard deviation of a crosswind gaussian concentration distribution. The Pasquill-Gifford correlations for  $\sigma_y$  as a function of downwind distance can be represented by the power law relation

$$\sigma_y = \delta x^\beta$$

where  $\beta = 0.9$  and  $\delta$  is approximately 0.33, 0.13 and 0.065 for B (unstable), D (neutral) and F (stable) atmospheres respectively. The rate of lateral spread with respect to downwind distance is then

$$\frac{dW_t}{dx} = 2.5 \delta \beta x^{\beta-1} \quad (48)$$

The ratio of Equation 46 to Equation 48 provides a measure of the relative importance of gravity spreading to atmospheric turbulence-induced lateral spreading.

Consider a heavy gas cloud formed over an LNG (assumed  $CH_4$ ) spill on water. For this case,  $g\Delta' = 3.9$  and  $W_o = 3.0 Q_i^{1/2}$ , assuming a constant boil-off flux of  $0.2 \text{ kg/m}^2 \text{ sec}$  for LNG on water. Using a value of  $\alpha = 1.0$ , and letting  $Z = (g\Delta' Q_i / u_a^3)$ , the ratio of Equation 46 to Equation 48 can then be written as

$$\frac{dW}{dW_t} = \frac{0.927 \delta^{-1.0} Z^{0.3} u_a^{-0.35}}{(4.5 X^{0.7} Z^{0.25} + 1.84 X^{-0.3} u_a^{0.75})^{1/3}} \quad (49)$$

where  $X$  is a nondimensionalized distance,  $X = x/W_o$ . For  $dW/dW_t = 1.0$ , solution of Equation 49 for  $X$  gives the downwind distance at which the lateral gravity-driven spreading rate has decreased to the passive spreading rate which would be expected due to atmospheric turbulence if no density-driven effects were present.

Table 3 gives the wind velocity and length scale  $Q_i g\Delta' / u_a^3$  for LNG spill-on-water tests conducted to date (no information is available on the Shell/Maplin Sands tests at the time of writing), which represent the best LNG-on-water field test data available. The downwind distance, expressed as  $X = x/W_o$ , at which the atmospheric turbulence-generated lateral spreading rate becomes equal to the gravity-driven lateral spreading rate indicates that lateral dispersion in the Bureau of Mines test series was dominated by atmospheric turbulence over almost the entire test measurement field. Only Esso Test 17, the Gadilla Tests (for which there is no concentration data) and DOE Test 8 show lateral dispersion clearly dominated by gravity spreading. DOE Test 9 indicates gravity-driven spreading dominating the instrument field, but the calculation is sensitive to the atmospheric stability class chosen. If an atmospheric stability class one category above (more unstable) is assumed, none of the DOE test series except Test 8 indicates gravity spread-dominated flow.

#### CLOSURE

A systematic evaluation of the models described here, by comparison with all of the experimental data presently available, by intercomparison of predictions for a range of scenarios which would encompass their intended use for risk evaluation and by comparison with laboratory tests and field tests now underway is being sponsored by the United States Coast Guard (43). Woodward et al. (44) have published a comparison of model predictions for selected LNG spills on water tests (Esso No. 11 and Esso No. 17) and isothermal dense gas release tests (Porton Downs Nos. 6, 8, and 20) using two K-theory models (ZEPHYR (34) and MARIAH (35)), the Germeles and Drake model (22), the Eidsvik model (19), and the Colenbrander (11) model. Fay (18) has compared the top hat profile models and suggested a simplified version of Eidsvik's entrainment model to correlate the available data from laboratory (including wind tunnel) tests and field tests. Fay's correlation of the test data was on the basis of model fit of three test parameters: peak

TABLE 3 - LNG-on-Water Field Test Conditions--Gravity Spread Analysis

	Bureau of Mines (40)			$u_a$	$Q_i$	$Q_i \Delta V u_a^3$	Stability Class	X	Downwind Centerline Sensor Position, x/W <sub>0</sub>
	No. 1	2.53	0.65	0.156	B	< 1	12.6, 31.5, 63.0		
	2	2.59	1.67	0.376	B	< 1	7.9, 19.7, 39.3		
	3	2.29	0.84	0.274	B	< 1	11.1, 27.7, 55.4		
	4	2.35	2.5	0.755	B	< 1	6.4, 16.1, 32.1		
	5	2.20	3.67	1.35	B	3	5.3, 13.3, 26.5		
	6	2.01	1.76	.85	B	2	7.7, 19.1, 38.3		
Gadilla (39)	1	5.1	30.0	0.89	D	40	None		
	2	3.9	78.0	5.15	D	313	None		
API/ESSO (41)	11	8.0	74.0	0.57	D	11	14, 18		
	17	4.0	70.0	4.3	D	255	10, 12		
DOE/Burro (42)	3	5.4	50.8	1.26	C/B	6/<1	2.7, 6.5, 18.7, 37.4		
	7	9.2	61.2	0.31	D	0/<1	2.4, 6.0, 17.0, 34.0		
	8	2.0	66.7	32.5	E/D	23000/4800	2.3, 5.7, 16.3, 32.7		
	9	6.0	76.7	1.38	D/C	46/5	2.2, 5.3, 15.2, 30.4		

ground level concentration as a function of time since the cloud formed, the distance from the cloud origin to the location of the peak concentration as a function of time, and the distance to peak concentration as a function of that concentration. Fay indicates that available field and wind tunnel heavy gas release test data can be adequately correlated (except for data taken very near the source of the cloud) with an entrainment sub-model of the form

$$w_e = \frac{u_*}{[K_1^{-2} + (K_2/Ri)^{-2}]^{1/2}}$$

with  $Ri = g\Delta'h/u_*^2$  and the following parameter values.

	$\alpha_1$ (in Eq. 5)	$K_1$	$K_2$
Isothermal releases	1.0	2.5	0.5
LNG-on-water releases	1.0	2.5	5.0

Fay found that the entrainment parameter  $K_2$  that best correlated the LNG-on-water spill test data (the Esso and Burro Series test data) was an order of magnitude greater than that required to fit the isothermal gas release data analyzed (Hall (45), Picknett (24), Neff and Meroney (46)). He suggested that the indicated increased vertical mixing rates for LNG clouds may be due to thermal convective flows resulting from the heat transfer from the earth's surface to the bottom layer of the cloud. It should be noted that Eidsvik's model includes provision for convection-generated turbulent vertical entrainment (it was not described herein) and that Woodward et al. reported the Eidsvik model gave fairly good predictions of the LNG spill on water test data for Esso tests 11, 16, 17 (using the model parameters reported earlier herein). However, Woodward et al. also reported fairly good prediction by the Colenbrander model of observed data for Esso Test 11 and 17 using the entrainment model parameters reported herein, and the Colenbrander model used did not provide for heat transfer to the cloud or for thermal convection-generated turbulence. The importance of heat transfer and thermal convection-induced turbulent mixing in non-isothermal clouds needs further study; some of the DOE Burro series data may be helpful in this regard. The test data correlation reported by Fay leads to predictions for the maximum downwind distance to the LFL for a 25,000 m<sup>3</sup> LNG spill on water in a 2.25 m/sec wind of about 7 km.

#### ACKNOWLEDGEMENTS

This review was prepared under United States Coast Guard Contract DTCG23-80-C-20029, entitled Development of Vapor Dispersion Models for Non-Neutrally Buoyant Gas Mixtures, with the University of Arkansas.

#### LITERATURE CITED

1. LNG Terminal Risk Assessment Study for Oxnard, California; prepared by Science Applications, Inc., La Jolla, California for Western LNG Terminal Company, Los Angeles, California, December 22, 1975.
2. Liquefied Energy Gases Safety; General Accounting Office Report to the Congress of the United States, July 31, 1978.

3. Safety Aspects of Liquefied Natural Gas in the Marine Environment, National Materials Advisory Board of the National Research Council, Report NMAB-354, June 1980.
4. Kaiser, G. D. and B. C. Walker, "Releases of Anhydrous Ammonia from Pressurized Containers--the Importance of Denser than Air Mixtures," *Atm. Env.* 12 (1978), p. 2289-2300.
5. Harris, C., "Analysis of Chlorine Accident Reports", presented at the Chlorine Institute's 21st Plant Manager's Seminar, Houston, Texas, February 15, 1978.
6. Liquefied Natural Gas, Views and Practices, Policy and Safety, U.S. Coast Guard Report CG-478, 1 February 1976.
7. Havens, J. A., An Assessment of Predictability of LNG Vapor Dispersion from Catastrophic Spills onto Water, *Journal of Hazardous Materials*, 3 (1980), p. 267-278.
8. Pasquill, F., *Atmospheric Diffusion*, Halstead Press Division of John Wiley and Sons, New York, 1974.
9. Turner, J. S., *Buoyancy Effects in Fluids*, Cambridge University Press, 1973.
10. te Riele, P. H. M., Atmospheric Dispersion of Heavy Gases Emitted at or Near Ground Level, Second International Symposium on Loss Prevention and Safety Promotion in the Process Industries, Heidelberg, Germany, 1977.
11. Colenbrander, G. W., A Mathematical Model for the Transient Behavior of Dense Vapor Clouds, Third International Symposium on Loss Prevention and Safety Promotion in the Process Industries, Basel, Switzerland, 1980.
12. Flothmann, D. and H. J. Nikodem, A Heavy Gas Dispersion Model with Continuous Transition from Gravity Spreading to Tracer Diffusion, in S. Hartwig, *Heavy Gas and Risk Assessment*, D. Reidel, Dordrecht, Holland, 1980.
13. Zeman, O., The Dynamics and Modeling of Heavier-than-Air, Cold Gas Releases, Lawrence Livermore Laboratory (University of California), Report UCRL-15224, April 17, 1980.
14. Rosenzweig, J. J., A Theoretical Model for the Dispersion of Negatively Buoyant Vapor Clouds, Ph.D. Dissertation, Massachusetts Institute of Technology, 1980.
15. Fannelop, T., The Dynamics of Heavy Gas Clouds, Report IFAG B-124, Division of Aero and Gas Dynamics, University of Trondheim, Norway, May 1980.
16. Blackmore, D. R., M. N. Herman, and J. L. Woodward, Heavy Gas Dispersion Models, to appear in *Journal of Hazardous Materials*.
17. Benjamin, T. B., Gravity Currents and Related Phenomena, *Journal of Fluid Mechanics*, 31, 1968, pp. 209-248.

18. Fay, J. Scale Effects in Liquefied Gas Vapor Dispersion, draft Final Report, DOE Contract DE-AC02-77 EV04204, September 1981.
19. Eidsvik, K. J., A Model for Heavy Gas Dispersion in the Atmosphere, *Atmospheric Environment*, 14, 1980, p. 769-777.
20. Tennekes, H. and J. L. Lumley, *A First Course in Turbulence*, MIT Press, 1972.
21. Van Ulden, A. P., On the Spreading of a Heavy Gas Released Near the Ground, First International Loss Symposium, The Hague, Netherlands, 1974.
22. Germeles, A. E. and E. M. Drake, Gravity Spreading and Atmospheric Dispersion of LNG Vapor Clouds, Fourth International Symposium on Transport of Hazardous Cargo by Sea and Inland Watersays, Jacksonville, Florida, 1975.
23. Lofquist, K., Flow and Stress Near an Interface Between Stratified Fluids, *Physics of Fluids*, 3, No. 2, March-April 1960.
24. Picknett, R. G., Field Experiments on the Behavior of Dense Clouds, Chemical Defence Establishment Report Ptn. IL 1154/78/1, Porton Downs, UK, September 1978.
25. Cox, R. A. and R. J. Carpenter, Further Development of a Dense Vapor Cloud Dispersion Model for Hazard Analysis, in S. Hartwig, *Heavy Gas and Risk Assessment*, D. Reidel, Dordrecht, Holland, 1979.
26. Taylor, R. J., J. Warner, and N. E. Bacon, Scale Length in Atmospheric Turbulence as Measured from an Aircraft, *Quarterly Journal Royal Meteorological Society*, 96 (1970), p. 750-755.
27. Arthur D. Little Company, Report on Hazard Models for Liquid Hydrocarbon Product Releases, to Esso Chemicals, Ltd., Ashley Place, London, March 1981.
28. Ooms, G., A. P. Mahieu, and F. Zelis, Plume Path of Heavy Gases, First Loss Prevention Symposium, The Hague, Netherlands, 1974.
29. McQuaid, J., Some Experiments on the Structure of Stably Stratified Shear Flows, Technical Paper P21, Safety in Mines Research Establishment, Sheffield UK, 1976.
30. Kato, H. and O. M. Phillips, On the Penetration of a Turbulent Layer into a Stratified Fluid, *Journal of Fluid Mechanics*, 37 (1969), p. 643-655.
31. Kantha, L. H., O. M. Phillips and R. S. Azad, "On Turbulent Entrainment at a Stable Density Interface", *Journal of Fluid Mechanics*, 79 (1977), p. 753-768.
32. Havens, J. A., A Description and Assessment of the SIGMET LNG Vapor Dispersion Model, U.S. Coast Guard Report CG-M-3-79, February 1979.
33. Science Applications, Inc., La Jolla, California.

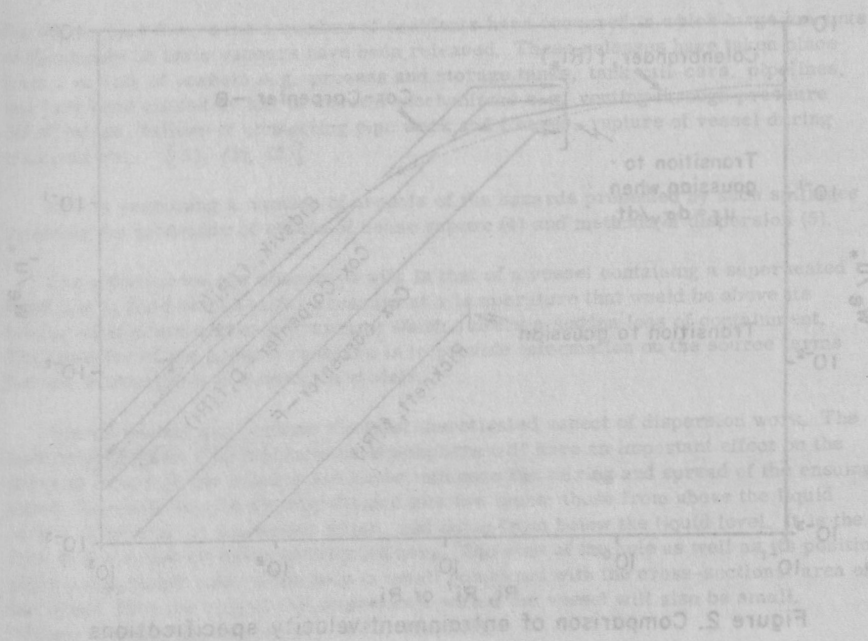
34. Energy Resources Company, La Jolla, California.
35. Deygon-Ra Company, La Jolla, California.
36. Hanna, S. R., A Method of Estimating Vertical Eddy Transport in the Planetary Boundary Layer Using Characteristics of the Vertical Velocity Spectrum, *Journal of the Atmospheric Sciences*, 25 (1968), p. 1026-1033.
37. Lumley, J. and H. Panofsky, *The Structure of Turbulence*, Interscience Publications, New York (1964).
38. Smith, T. B. and B. L. Niemann, *Shoreline Diffusion Program: Ocean-side, California, Vol. I*, Technical Report, by Meteorology Research, Inc. To Desert Test Center, Ft. Douglas, Utah, Contract No. DA-42-007-ACM-180(R).
39. Kneebone, A. and L. R. Prew, *Shipboard Jettison Tests of LNG onto the Sea*, Proceedings of the Fourth International LNG Conference, Amsterdam (1974).
40. Burgess, D., J. Biordi, and J. Murphy, *Hazards of Spillage of LNG into Water*, PMSRC Report No. 4177, prepared for U.S. Coast Guard Hazardous Materials Division, Washington DC, September 1972.
41. Feldbauer, G. F., J. J. Heigel, W. McQueen, R. H. Whipp, and W. G. May, "Spills of LNG on Water--Vaporization and Downwind Drift of Combustible Mixtures," Esso Research and Engineering Report No. EE61D-72 (Performed for the American Petroleum Institute), 24 November 1972.
42. Koopman, R. P., Lawrence Livermore Laboratories, personal communication.
43. Havens, J. A., contract DTCG23-80-C-20029, Development of Vapor Dispersion Models for Non-Neutrally Buoyant Gas Mixtures, with the University of Arkansas.
44. Woodward, J. L., J. A. Havens, W. C. McBryde, and J. R. Taft, A Comparison with Experimental Data of Several Models for Dispersion of Heavy Vapor Clouds, 12th International NATO Technical Meeting on Air Pollution Modeling and its Application, Menlo Park, California, August 25-28, 1981.
45. Hall, D. J., Experiments on a Model of an Escape of Heavy Gas, Warren Springs Laboratory, Stevenage, England, Reports LR 217(AP), 1976 and LR312(AP) 1979.
46. Neff, D. E. and R. N. Meroney, *The Behavior of LNG Vapor Clouds*, draft Final Report CEF81-S2DEN-RNMI to the Gas Research Institute, Contract No. 5014-352-2030, July 1981.

## SYMBOLS USED

$A_F$	= cloud frontal area ( $m^2$ )
$A_T$	= cloud top area ( $m^2$ )
$a, b$	= constants in self-similar concentration profiles
$B$	= effective width of gas plume, Equation 39 (m)
$b$	= half-width of horizontally homogeneous central section of gas plume, used in Colenbrander's model (m)
$C_F$	= surface-friction drag coefficient
$c$	= concentration ( $kg/m^3$ )
$C_A$	= centerline, ground level, concentration ( $kg/m^3$ )
$c_f$	= frontal entrainment parameter
$c_1$	= top entrainment parameter in Equation 12
$c_2$	= top entrainment parameter in Equation 13
$c_3$	= top entrainment parameter in Equation 14
$D$	= source diameter (m)
$g$	= acceleration of gravity ( $m^2/s$ )
$h$	= height or depth of density intrusion or cloud (m)
$h_{eff}$	= effective cloud depth, Equation 34 (m)
$K_V$	= vertical eddy diffusivity ( $m^2/s$ )
$k$	= von Karman's constant, 0.35
$L$	= turbulence scale length (m)
$n$	= shape-dependent constant in Equation 18
$Q_i$	= steady gas volumetric release rate ( $m^3/s$ )
$Ri$	= Richardson number, $g\Delta h/u_*^2$ or $g\Delta' h/u_*^2$
$Ri'$	= Richardson number, $g\Delta h/w^2$
$Ri''$	= Richardson number, $g\Delta' L/u_1^2$
$Ri_*$	= Richardson number, $g\Delta' h_{eff}/u_*^2$
$s_y$	= horizontal concentration scaling parameter used in Colenbrander model (m)

- $s_z$  = vertical concentration scaling parameter used in Colenbrander model (m)  
 $T$  = temperature (K)  
 $t$  = time (s)  
 $u$  = average flow velocity (m/s)  
 $u_a$  = characteristic wind velocity, such as velocity at a specified height or vertically averaged (m/s)  
 $u_e$  = horizontal entrainment velocity (m/s)  
 $u_{eff}$  = effective cloud advection velocity, Equation 35 (m/s)  
 $u_f$  = gravity spreading front velocity (m/s)  
 $u_{f0}$  = gravity spreading front velocity at  $t = 0$  (m/s)  
 $u_g$  = gravity spreading velocity (m/s)  
 $u_x$  = wind velocity, along x direction (m/s)  
 $u_0$  = wind velocity measured at  $z = z_0$  (m/s)  
 $u_1$  = horizontal r.m.s. turbulence velocity in Equation 25 (m/s)  
 $u_*$  = friction velocity (m/s)  
 $V$  = volume of gas cloud ( $m^3$ )  
 $\dot{V}$  = rate of change of cloud volume ( $m^3/s$ )  
 $\dot{V}_a$  = volumetric rate of air entrainment ( $m^3/s$ )  
 $W$  = lateral width of gravity spreading plume (m)  
 $W_t$  = lateral width of atmospheric turbulence-dominated plume  
 $W_0$  = side length of square area equivalent to circle of diameter  $D$  (m)  
 $w$  = characteristic turbulent entrainment velocity in Equation 16 (m/s)  
 $w_e$  = vertical entrainment velocity (m/s)  
 $x, y, z$  = cartesian coordinates (m)  
 $x_s, y_s, z_s$  = cartesian coordinate length scale factors (m)  
 $z_0$  = reference height in wind velocity profile specification (m)

- $\alpha_1$  = constant in density intrusion spreading relation  
 $\alpha$  = constant in power law wind profile  
 $\Delta$  =  $(\rho_g - \rho_a)/\rho_g$   
 $\Delta'$  =  $(\rho_g - \rho_a)/\rho_a$   
 $\phi(Ri_*)$  = function describing influence of density stratification on vertical diffusion, Equation 32  
 $\sigma_w$  = standard deviation of the vertical fluctuation of the wind velocity (m/s)  
 $\sigma_y$  = Pasquill-Gifford horizontal dispersion parameter  
 $\sigma_y$  = Pasquill-Gifford lateral dispersion coefficient  
 $\rho_a$  = density of air ( $kg/m^3$ )  
 $\rho_g$  = density of gas-air mixture ( $kg/m^3$ )



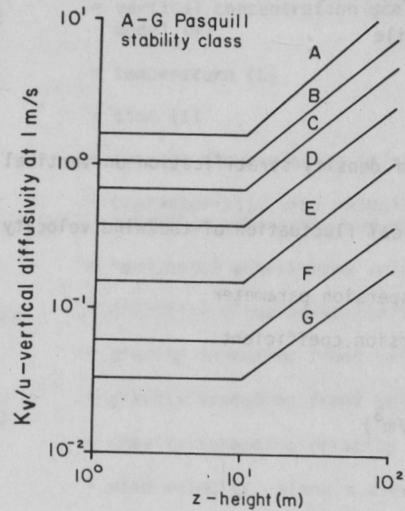


Figure 1. SIGMET vertical diffusivity specification

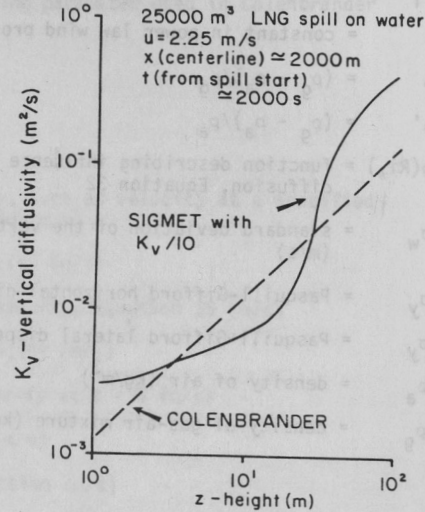


Figure 3. Comparison of SIGMET and COLENBRANDER diffusivity specifications

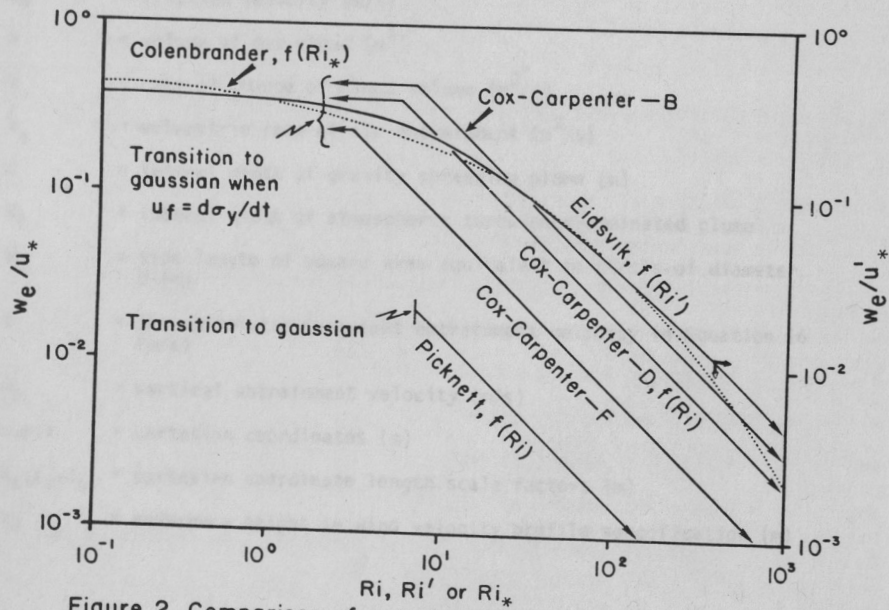


Figure 2. Comparison of entrainment velocity specifications

SUDDEN DISCHARGE OF A SUPERHEATED FLUID TO ATMOSPHERE

B. Fletcher\*

Experiments have been carried out on the discharge of superheated fluids (Refrigerants 11 and 114) from an orifice formed in the vapour space of a closed vessel. Measurements have been made both when the vessel top is removed completely and when discharge takes place through vent areas of the order of one per cent of the vessel cross-sectional area.

INTRODUCTION

During the past few years a number of accidents have occurred in which large amounts of flammable or toxic vapours have been released. These releases have taken place from a variety of vessels e.g. process and storage tanks, tank rail-cars, pipelines, and have been caused by any of several mechanisms e.g. venting through pressure relief valves, failure of connecting pipe work and flanges, rupture of vessel during transport etc. [(1), (2), (3)]

HSE is examining a number of aspects of the hazards presented by such spillages including the behaviour of clouds of dense vapour (4) and methods of dispersion (5).

The situation we are concerned with is that of a vessel containing a superheated fluid (i.e. a fluid stored under pressure at a temperature that would be above its boiling point at atmospheric pressure) which suffers a sudden loss of containment. The objective of the present research is to provide information on the source terms for use in atmospheric dispersion models.

Source models are perhaps the least investigated aspect of dispersion work. The method of release of a fluid into the atmosphere will have an important effect on the physical nature of the release and hence influence the mixing and spread of the ensuing cloud. Releases may be broadly divided into two types: those from above the liquid level i.e. venting of the vapour space, and those from below the liquid level. It is the first of these that attention is directed here. The size of the hole as well as its position plays a significant role; if the hole is small compared with the cross-sectional area of the vessel then the rate of fall of pressure within the vessel will also be small.

\*Safety Engineering Laboratory, HSE, Sheffield.